Thermoelastic Stability Behavior of Curvilinear Fiber-Reinforced Composite Laminates With Different Boundary Conditions

Ganapathi Manickam, Anirudh Bharath, Aditya Narayan Das, Anant Chandra, Pradyumna Barua
School of Mechanical Engineering, Vellore Institute of Technology, Vellore 632014, India

In this article, the thermoelastic stability behavior of curvilinear fiber-reinforced composite laminates is investigated using a shear flexible plate theory. The laminate is composed of layers that make use of curvilinear fibers to create spatial variation of stiffness due to the continuous change of fiber orientation within the lamina. Such composite laminates, subjected to different thermal loads like uniform and non-uniform temperature distributions, are considered in this analysis. The governing equations obtained using the principle of minimization of total potential energy, are solved for evaluating the critical buckling temperature. The displacement fields of pre-buckling of the laminate are evaluated before proceeding for the thermal buckling analysis. The formulation is checked against available solutions in the literature. A detailed parametric study considering important design parameters such as curvilinear fiber angles, lay-up, thickness ratio, coefficients of thermal expansion, and modular ratio on the thermoelastic stability/buckling behavior of composite laminates is made. The present analysis highlights the substantial change in the critical buckling loads due to the curvilinear fiber angles, lay-up and boundary conditions. The new results presented here for curvilinear fiber-reinforced composite laminate with clamped/mixed boundary conditions may be useful in assessing similar studies based on higher-order theories or other numerical studies.
POLYM. COMPOS., 2018.

HIGHLIGHTS

- Investigation of thermoelastic buckling of curvilinear fiber-reinforced composite laminates.
- Laminates with curvilinear fibers resulting in spatially variable stiffness composite plates.
- Detailed investigation made assuming various design parameters and thermal fields.
- New results for the thermal stability of such laminates with different boundary conditions.

Correspondence to: M. Ganapathi; e-mail: ganapathi.m@vit.ac.in
DOI 10.1002/pc.25116
Published online in Wiley Online Library (wileyonlinelibrary.com).

INTRODUCTION

The use of advanced composite materials in many engineering fields has been growing rapidly due to their excellent properties. Furthermore, the best structural design using such materials can be obtained based on numerical simulations using classical/shear deformation structural theory. Various shear deformation theories are considered for the accurate prediction of either global or local behavior of fiber-reinforced polymer composite structures. The conventional composite laminate with layers making use of spatially straight fibers leads to constant stiffness over the laminate. Various applications and studies pertaining to such laminated composite plates/shells are reviewed and well documented in the literature [1–4].

The laminated composite structures with varying stiffness have received considerable attention among researchers as they may lead to better and more efficient structural designs. The stiffness of the composite laminate can be altered by varying the volume fraction of fiber, fiber spacing, dropping, or adding plies to the laminate, and attaching discrete stiffeners to the laminate. Recent advancement in manufacturing process has demonstrated the possibility of realizing the curvilinear fiber-reinforced polymer composite laminate wherein the fiber angle can be spatially varied in each layer leading to a type of variable stiffness composite laminate (VSCL). The advantage of using such VSCL is that it can create the possibility of altering the load paths or non-uniform stress distribution in the laminate. This type of composite laminate is further shown to have greater resilience to buckling, better thermal properties, and found to be flexible in the sense that its deformation under different loadings can be controlled to produce favorable geometric configuration. For instance, Murugan and Friswell [5] have investigated the application of these composites in morphing wing structures. In this study, composite laminates with curvilinear fiber paths have been examined to address the conflicting structural requirement of low in-plane stiffness and high out of plane bending stiffness.

The available literature related to the VSCLs with curvilinear fibers is mainly dealt with the vibration, optimization,

mechanical buckling and postbuckling analyses. A study on the use of curvilinear fibers in improving the mechanical buckling resistance of composite plates is firstly conducted by Hyer and Lee [6] and focused on strengthening of plate with holes based on sensitivity analysis. Hao et al. [7] have analyzed the buckling of VSCL employing first-order shear deformation theory coupled with isogeometric analysis. The static stress analysis is carried out prior to the buckling study to improve the accuracy of the solutions. A variable-kinematic model for buckling and vibration analyses of variable stiffness composite plates is introduced in the work of Vescovini and Dozio [8]. The formulation developed in the context of a variational framework together with the Ritz method has been adopted to analyze the problem. Marouene et al. [9] have conducted the experimental study on the stability behavior of VSCL including panels containing gaps and overlaps due the placement of fibers.

The study of postbuckling behavior of laminates with curvilinear fibers under compressive loading has been attempted by Madeo et al. [10] using Koiter's approach in conjunction with a mixed finite element method. White et al. [11] have performed the postbuckling of such curved composite panels. Setoodeh et al. [12] have investigated the optimization of laminates to enhance the buckling strength by updating the fiber angles in the discretized domains based on the deformation pattern of laminates. Ghiasi et al. [13] have optimized the stacking sequence of the layers for improving the compressive strength of plate. Falcó et al. [14] have presented a detailed analytical method to predict the failure characteristics of a ply based on the fiber path and curvature. The influence of variation in the material properties was examined by Nik et al. [15] while dealing with the optimization of VSCLs. Similar study is made considering laminate with induced defects under compressive load by Venkatachari et al. [16]. Wu et al. [17] have recently dealt with the optimization of postbuckling behavior of panel with variable tow angle and obtained the first-level optimal solutions in terms of lamination parameters. The effect of various structural models in predicting the mechanical and thermal behavior of curvilinear fiber-reinforced composite laminates is assessed in the work of Venkatachari et al. [18]. The available research work related to the mechanical behavior of curvilinear fiber-based composite laminates is recently reviewed and documented in Ref. [19].

The research work dealing with the vibration and dynamic response analysis of VSCLs with curvilinear fibers available in the literature are briefly discussed here. The linear and non-linear vibration analyses of curvilinear fiber composite panels are examined by Abdalla et al. [20], and Ribeiro and Akhavan [21] considering different geometric configurations. Houmat [22] has studied the forced vibrations of plates whereas Ribeiro and Stoykov [23] have simulated the free and forced vibration characteristics of composite cylindrical shells. The hygrothermal effect on the free vibration of such laminates with cut-out has been attempted by Venkatachari et al. [24] and the variation of natural frequency is highlighted through the fiber tow angles and the cut-out ratio. Tan and Nie [25] have carried out the free and forced vibrations of variable thickness composite annular thin plates with elastically restrained edges employing the method of weighted residuals. Loja et al. [26] have analyzed the dynamic instability of VSCL subjected to periodic inplane load using the Rayleigh-Ritz method.

In general, the structural elements such as plates and panels may get exposed to the thermal environment. For instance, when these structures exposed to supersonic or hypersonic airflow, high temperature may be generated over the surface due to the aerodynamic heating and can be of non-uniform distributions. Therefore, it is important to maximize the stiffness of the structure while minimizing the weight of the composite structures under thermal environment. Such studies pertaining to the conventional composite laminates making use of spatially straight fibers have received significant importance in the literature [27,28]. Some of the notable contributions are discussed here. Chen et al. [29] have examined the thermal buckling of various configurations of laminated composite plates using first-order shear deformation theory whereas Ganapathi and Touratier [30] have carried out the postbuckling of laminates assuming different temperature loads. Kant and Babu [31] have solved the stability of skew fiber-reinforced composite/sandwich flat panels under thermal loads employing various high-order shear deformation theories whereas Vosoughi et al. [32] have extended the investigation of the postbuckling of such plates. The dynamic response analysis of composite laminates under thermal and mechanical loadings is highlighted in the work Makhecha et al. [33] wherein a higher-order shear deformation theory accounting for the thickness stretching effect has been introduced. The influence of material properties and lay-up sequences on the thermo-elastic stability characteristics of composite plates is brought out in the work of Shiau et al. [34]. Recently, using the approach of sublaminates in conjunction with variable-kinematic formulation, the thermal buckling analysis of composite plates and sandwich panels is carried out in Ref. 35 whereas Cetkovic [36] has employed a layer-wise displacement model while studying the similar class of problem. Singha et al. [37] have considered the postbuckling of composite laminates with different boundary conditions. Patel et al. [38] have worked on the thermo-flexural analysis of thick laminates of bi-modulus composite materials whereas the study of hygrothermal elastic stability of thick plate is discussed in Ref. 39. The research work on the thermal buckling and post buckling of functionally graded composite laminates have also received considerable importance in the literature [40–45] using analytical/numerical approaches. Thermal buckling analysis of functionally graded material plates with internal defects is performed by Yu et al. [46] using an extended isogeometric analysis. The effect of through thickness temperature variation on the stability of such plates has been brought out in Ref. 47. It is further observed that a large

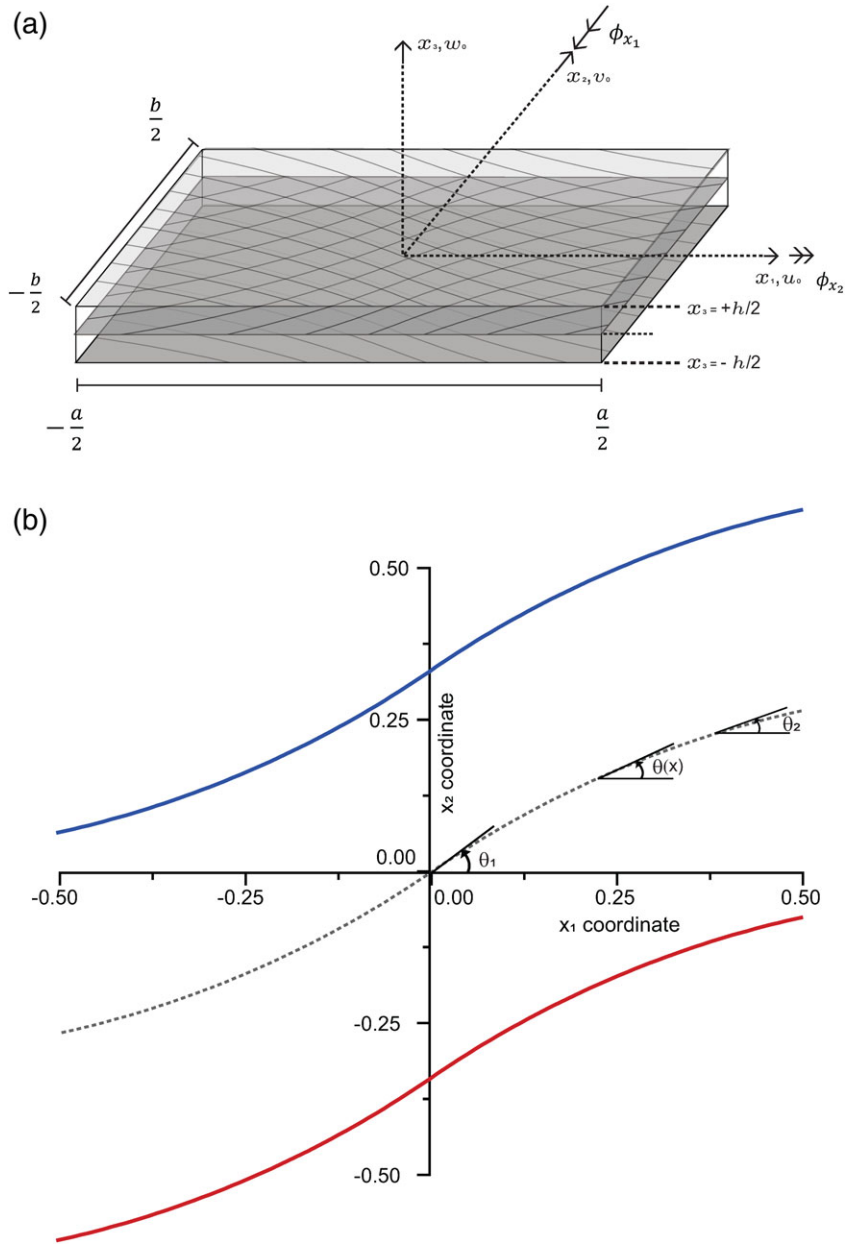

FIG. 1. (a) Plate coordinates, (b) Curvilinear fiber-reinforced composite laminate fibers. [Color figure can be viewed at wileyonlinelibrary.com]

amount of literature with reference to the thermal stress and buckling has been dealt with the simple supported boundary conditions. However, such studies considering complex boundary conditions, for instance, clamped conditions or arbitrary boundary conditions are sparsely treated in the literature [48,49]. Furthermore, it can be opined from the available studies that a comprehensive insight into the thermo-structural behavior of curvilinear fiber-reinforced composite structures appears to be missing in the literature.

Here, we have focused on the thermoelastic stability/buckling of curvilinear fiber-reinforced composite laminates with various boundary conditions under uniform and non-uniform temperature fields. The mathematical model developed based on first-order shear flexible theory is solved using finite element approach employing an eight-noded C^0 quadrilateral field-consistent plate element [50,51]. Attempts have been made to examine the influence of the range of fiber orientations at the middle and edge of the laminae in maximizing the buckling stiffness of the laminate. Two types of temperature distributions, such as, uniform and sinusoidal temperature distributions are assumed here in present analysis. Since pre-buckling deformation may not be applicable for buckling of laminates under non-uniform temperature loading cases, thermal stress analysis is firstly carried out before evaluating the actual buckling values. The influence of the important geometrical and material parameters such as lay-up sequence, number of layers, thickness ratio, material properties and

boundary conditions on the thermal buckling loads of curvilinear fiber-reinforced composite laminates are highlighted.

The article is structured with "Theoretical Formulation" Section presenting the theoretical formulation accounting for shear deformation, variation of curvilinear fiber and the governing equation. "Results and Discussion" Section deals with results and discussion based on systematic parametric study on the buckling behavior; last, "Conclusion" Section concludes the article based on the assessment of various design parameters.

THEORETICAL FORMULATION

Considering a composite laminate having length a, width b, thickness h, and n layers with x_1, x_2 as coordinates along the in-plane directions and x_3 through the thickness direction (see Fig. 1a), the displacement functions (u, v, w) at any position from the mid-surface are considered as function of mid-plane displacements (u_0, v_0, w_0), and independent rotations (ϕ_{x_1} and ϕ_{x_2}) of the normal in the transverse planes (x_1x_3 and x_2x_3) respectively as

$$\begin{Bmatrix} u(x_1,x_2,x_3) \\ v(x_1,x_2,x_3) \\ w(x_1,x_2,x_3) \end{Bmatrix} = \begin{Bmatrix} u_0(x_1,x_2) \\ v_0(x_1,x_2) \\ w_0(x_1,x_2) \end{Bmatrix} + x_3 \begin{Bmatrix} \phi_{x_1}(x_1,x_2) \\ \phi_{x_2}(x_1,x_2) \\ 0 \end{Bmatrix} \quad (1)$$

The different strain vectors such as the membrane, bending and transverse shear strains, and thermal strains ($\{\varepsilon_m\}$, $\{\varepsilon_b\}$, $\{\varepsilon_s\}$,and$\{\varepsilon_t\}$) are respectively, presented in the bending analysis composite laminate based on the assumed displacement kinematics as

$$\begin{aligned} \{\varepsilon\} &= \{\varepsilon_{x_1x_1}\ \varepsilon_{x_2x_2}\ \gamma_{x_1x_2}\ \gamma_{x_1x_3}\ \gamma_{x_2x_3}\}^T \\ &= \begin{Bmatrix} \varepsilon_m \\ 0 \end{Bmatrix} + x_3 \begin{Bmatrix} \varepsilon_b \\ 0 \end{Bmatrix} + \begin{Bmatrix} 0 \\ \varepsilon_s \end{Bmatrix} - \begin{Bmatrix} \varepsilon_t \\ 0 \end{Bmatrix} \end{aligned} \quad (2)$$

where.

$$\begin{aligned} \{\varepsilon_m\} &= \begin{Bmatrix} u_{0,x_1} \\ v_{0,x_2} \\ v_{0,x_2} + u_{0,x_1} \end{Bmatrix}; \{\varepsilon_b\} = \begin{Bmatrix} \kappa_{x_1} \\ \kappa_{x_2} \\ \kappa_{x_1x_2} \end{Bmatrix} \\ &= \begin{Bmatrix} \phi_{x_1,x_1} \\ \phi_{x_2,x_2} \\ \phi_{x_1,x_2} + \phi_{x_2,x_1} \end{Bmatrix}; \{\varepsilon_t\} = \begin{Bmatrix} \varepsilon^t_{x_1} \\ \varepsilon^t_{x_2} \\ \varepsilon^t_{x_1x_2} \end{Bmatrix} = \begin{Bmatrix} \alpha_{11} \\ \alpha_{22} \\ 2\alpha_{12} \end{Bmatrix} \Delta T \end{aligned} \quad (3a)$$

$$\{\varepsilon_s\} = \begin{Bmatrix} \gamma_{x_1x_3} \\ \gamma_{x_2x_3} \end{Bmatrix} = \begin{Bmatrix} w_{0,x_1} + \phi_{x_1} \\ w_{0,x_2} + \phi_{x_2} \end{Bmatrix} \quad (3b)$$

Here, $()_{,x_1}$ and $()_{,x_2}$ represent the partial differentiation with respect to x_1 and x_2; respectively. $\Delta T(=T - T_0)$is temperature rise from the reference temperature T_0 at which there is no thermal strains;α_{11}, α_{22} are the coefficients of thermal expansion in the principle material directions.

The constitutive equation for a kth layer in the laminate can be represented as

TABLE 1. Convergence study of critical thermal buckling parameter ($\lambda_{cr}\alpha_{11}10^3$) for a clamped four-layered antisymmetric $[\pm(\theta_1/\theta_2)]_4$square laminates ($a/h$ = 10, 20, 40)

		Thickness Ratio (a/h)		
$[\pm(\theta_1/\theta_2)]_4$	Mesh	10	20	40
[±(15/15)]	2 × 2	10.5840	2.9806	1.0314
	4 × 4	8.3007	4.9791	1.7284
	6 × 6	9.8999	4.9827	1.7073
	8 × 8	9.8954	4.9770	1.7026
	16 × 16	9.8903	4.9724	1.7001
[±(15/45)]	2 × 2	10.1670	2.6889	0.9453
	4 × 4	10.9630	5.2421	1.6992
	6 × 6	11.2560	5.1901	1.6680
	8 × 8	11.2440	5.1769	1.6619
	16 × 16	11.2350	5.1693	1.6586
[±(15/75)]	2 × 2	5.1640	3.1388	0.9095
	4 × 4	11.7300	5.5041	1.7731
	6 × 6	11.4240	5.6156	1.7274
	8 × 8	11.5080	5.5969	1.7173
	16 × 16	11.5440	5.5862	1.7125

$$\begin{aligned} \{\sigma\} &= \{\sigma_{x_1x_1}\sigma_{x_2x_2}\tau_{x_1x_2}\tau_{x_1x_3}\tau_{x_2x_3}\}^T \\ &= \left[\overline{Q}_k\right]\{\varepsilon_{x_1x_1}\varepsilon_{x_2x_2}\gamma_{x_1x_2}\gamma_{x_1x_3}\gamma_{x_2x_3}\}^T \end{aligned} \quad (4)$$

Here the superscript T represents the transpose of a vector or matrix; $\{\sigma\}$ is the stress vector; the stiffness matix $\left[\overline{Q}_k\right]$ of kth layer is obtained with respect to laminate axes and can be derived from the $[Q_k]$ provided with respect to fiber directions [52]. It can be noted that $[Q_k]$ may vary along the surface of the plane $x_1x_2$within a lamina if the fiber angle θdepends on the spatial co-ordinates.

Unlike in the conventional laminates with rectilinear fibers, the fiber paths in the variable stiffness composite panels introducing curvilinear fibers have to be defined by variable orientation angle. It is presumed that the reference fiber path orientation varies linearly with x_1 having orientation angles θ_0 and θ_1 at the center and edge of the lamina (x_1=a/2), respectively, as shown in Fig. 1b. The lamina made of such fibers is referred as $\langle\theta_1\theta_2\rangle$. The fiber path function x_2 and the associated orientation angle $\theta(x_1)$that permit for a wide range of properties are defined for the kth lamina as [17,18,20].

$$x_2 = \begin{cases} \frac{a}{2(\theta_1-\theta_0)}\{-\ln(\cos\theta_0) + \ln[\cos(\theta_0 - 2(\theta_1-\theta_0)x_1/a]\} & -\frac{a}{2} \le x_1 \le 0 \\ \frac{a}{2(\theta_1-\theta_0)}\{\ln(\cos\theta_0) - \ln[\cos(\theta_0 + 2(\theta_1-\theta_0)x_1/a]\} & 0 \le x_1 \le \frac{a}{2} \end{cases} \quad (5)$$

$$\theta(x_1) = \begin{cases} -\frac{2}{a}(\theta_2-\theta_1)x_1 + \theta_1 & -\frac{a}{2} \le x_1 \le 0 \\ \frac{2}{a}(\theta_2-\theta_1)x_1 + \theta_1 & 0 \le x_1 \le \frac{a}{2} \end{cases} \quad (6)$$

The curvature κ for a curvilinear fiber path is defined as.

$$\kappa = \frac{\frac{d^2x_2}{dx_1^2}}{\left[1 + \left(\frac{dx_2}{dx_1}\right)^2\right]^{3/2}} \quad (7)$$

DOI 10.1002/pc

TABLE 2. Comparison of thermal-bending results (deflection and stresses) with analytical results [48] for SSCC boundary conditions.

Layer	a/h	$\bar{w}\,(10w(0,0,0)h/(a_{11}b^2\bar{\lambda}))$			$\bar{\sigma}_{x_1x_1}\,(10\sigma_{x_1x_1}(0,0,-h/2)h/(E_{22}a_{11}b\bar{\lambda}))$			$\bar{\sigma}_{x_2x_2}\,(-10\sigma_{x_2x_2}(0,0h/2)h/(E_{22}a_{11}b\bar{\lambda}))$			$\bar{\sigma}_{x_2x_3}\,(10\sigma_{x_2x_3}(0,b/2,0)h/(E_{22}a_{11}b\bar{\lambda}))$		
			Ref. 48			Ref. 48			Ref. 48			Ref. 48	
		Present	FSDT	HSDT	Present	FSDT	HSDT	Present	FSDT	HSDT	Present	FSDT	HSDT
0	10	0.2915	0.2912	0.2871	7.7716	–	–	1.3762	–	–	0.0878	0.0601	0.0903
0/90		0.5310	0.5307	0.5164	1.0953	–	–	3.3544	3.3902	3.6908	0.0892	–	–
0/90/0		0.3215	0.3211	0.3275	7.6566	7.7020	7.5416	1.3719	–	–	0.1446	–	–
0	5	0.3921	0.3915	0.3663	15.7214	–	–	2.4042	–	–	0.2868	0.1921	0.2909
0/90		0.6236	0.6231	0.5814	13.2957	–	–	3.5445	3.6323	5.0886	0.2761	–	–
0/90/0		0.4586	0.4578	0.4558	15.5914	15.6783	14.6976	2.4303	–	–	0.3811	–	–

In general, to create laminates with curvilinear fibers, it is essential to curve the tow paths as a part of manufacturing process. If a tow is curved too much, then it is possible that a kink will develop in the fiber, thus leading to defect /damage in ply. To avoid kinking, it is a general practice followed in the manufacturing process by limiting the magnitude of the maximum curvature value for any ply in the direction of fiber path less than certain allowable value. For instance, at each point along the fiber path, the magnitude of the curvature κ is limited to <3.28 m^{-1} [17,18,20,22]. In case the fiber curvature constraint is not satisfied along the fiber path direction, such ply is eliminated for manufacturing.

The strain energy function U pertaining to the VSCL is expressed by,

$$U(\delta)=\frac{1}{2}\int\int\left[\sum_{k=1}^{L}\int_{h_k}^{h_{k+1}}\{\sigma\}^T\{\varepsilon\}dx_3\right]dx_1dx_2 \tag{8}$$

where h_k, h_{k+1} are the x_3 coordinates of laminate corresponding to the bottom and top surfaces of the kth layer. δ is the vector of the degrees of freedom associated to the displacement field in a finite element discretization.

Substituting *Eq. 3* into the constitutive relation *Eq. 4*, one can rewrite strain energy functional U as

$$U(\delta)=\frac{1}{2}\{\delta\}^T[K]\{\delta\}-\{\delta\}^T[\{N^t\}+\{M^t\}] \tag{9}$$

where $[K]$ presents the stiffness matrix; $\{N^t\}$ & $\{M^t\}$ are the thermal load vectors due to thermal stress resultants and moment resultants, respectively.

The composite panel is subjected to temperature field and this, in turn, results in thermal stress and moment resultants $\{N^t\}=\{N^{th}_{x_1x_1}N^{th}_{x_2x_2}N^{th}_{x_1x_2}\}$ and $\{M^t\}=\{M^{th}_{x_1x_1}M^{th}_{x_2x_2}M^{th}_{x_1x_2}\}$., respectively. Thus, the potential energy (V) due to the thermal pre-buckling stresses developed under assumed thermal field can be written as

$$\begin{aligned}V(\delta)=&\frac{1}{2}\int\int\left[N^{th}_{x_1x_1}\left(\frac{\partial w}{\partial x_1}\right)^2+N^{th}_{x_2x_2}\left(\frac{\partial w}{\partial x_2}\right)^2+2N^{th}_{x_1x_2}\left(\frac{\partial w}{\partial x_1}\right)\left(\frac{\partial w}{\partial x_2}\right)\right]dx_1dx_2\\&+\frac{h^3}{24}\int\int\left[N^{th}_{x_1x_1}\left\{\left(\frac{\partial\phi_{x_1}}{\partial x_1}\right)^2+\left(\frac{\partial\phi_{x_2}}{\partial x_1}\right)^2\right\}\right.\\&\left.+N^{th}_{x_2x_2}\left\{\left(\frac{\partial\phi_{x_1}}{\partial x_2}\right)^2+\left(\frac{\partial\phi_{x_2}}{\partial x_2}\right)^2\right\}\right]dx_1dx_2\\&+\frac{h^3}{24}\int\int\left[2N^{th}_{x_1x_2}\left\{\left(\frac{\partial\phi_{x_1}}{\partial x_1}\right)\left(\frac{\partial\phi_{x_1}}{\partial x_2}\right)+\left(\frac{\partial\phi_{x_2}}{\partial x_1}\right)\left(\frac{\partial\phi_{x_2}}{\partial x_2}\right)\right\}\right]dx_1dx_2\\&=\frac{1}{2}\{\delta\}^T[K_G]\{\delta\}\end{aligned} \tag{10}$$

where $[\boldsymbol{K_G}]$ is the geometric stiffness matrix associated with the in-plane thermal stress state.

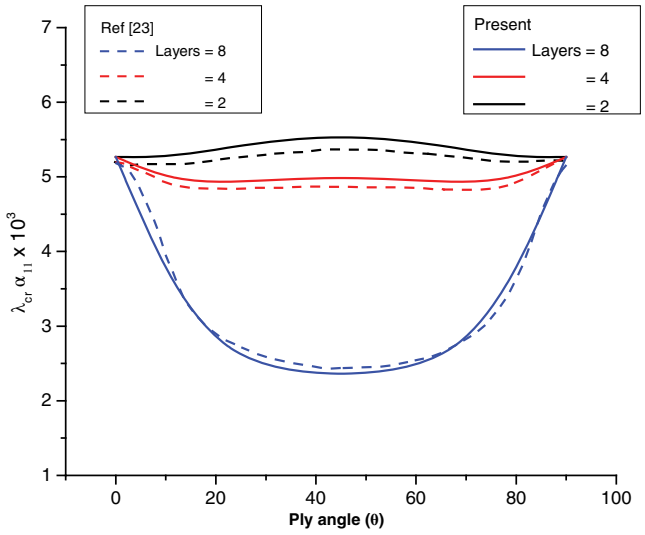

FIG. 2. Comparison of thermal buckling parameter ($\lambda_{cr}\ \alpha_{11}10^3$) for the clamped multi-layered square laminates (a/h = 10) with straight fibers under uniform thermal load. [Color figure can be viewed at wileyonlinelibrary.com]

For the thermo-flexural case, the minimization of the energy functional given in *Eq. 9* leads to the governing equations as outlined in Zienkiewicz and Taylor [53].

$$[[K]]\{\delta\} = \{N^t\} + \{M^t\} \tag{11}$$

The displacement field of pre-buckling of the laminate can be evaluated solving *Eq. 9*. For thermo-elastic buckling case, the equilibrium equation is obtained by minimizing the total potential energy associated with *Eqs. 9* and *10*, $\delta U_T = \delta(U - V) = 0$ as follows:

$$[[K] + \lambda[K_G]]\{\delta\} = \{0\} \tag{12}$$

where $\lambda$is the critical temperature rise which is the product of the eigenvalue and the initial guessed value of the temperature for the evaluation of in-plane thermal stress resultants $\{N^t\}$ as required in *Eq. 10*.

The governing equlibrium equations given in *Eq. 12* is treated as an eigenvalue problem. It is numerically sloved using standard eigenvalue approach and finite element procedure with a C^0 continuous, eight-noded serendipity quadrilateral shear flexible plate element developed in [50,51]. There are five nodal degrees of freedom per node (u_0, v_0, w_0, ϕ_{x_1}, ϕ_{x_2}) in the element as observed from the displacement kinematic function given in Eq. *1*. Since the element employed here is formulated using field-consistency approach, the element is free from shear locking syndrome and does not require reduced numerical integration scheme to alleviate the shear locking phenomenon and exact integration is numerically carried out. The element has a good convergence characteristic and no spurious rigid body modes.

RESULTS AND DISCUSSION

In this work, the investigation is focused on the thermo-elastic stability behavior of curvilinear fiber-reinforced composite laminates with different boundary conditions. Since the formulation is based on the shear deformation effects, the numerical experimentation is conducted for fairly thick to thin laminates. Exact numerical integration scheme is used as the element employed is derived through field-consistency approach. The shear correction factor is taken as $k_1^2 = k_2^2 = 5/6$. The influences of various geometric and material parameters like the thickness and aspect ratios, material anisotropy, lay-up, temperature distribution and curvilinear fiber angles at center as well as at the edge of the laminate on the thermal buckling characteristics of curvilinear fiber-based composite plates are discussed. The effect of various boundary conditions is also investigated. Unless specified otherwise, the material properties considered in the present study are as follows [29]:

$$E_{11}/E_{22} = 40;\ G_{12}/E_{22} = G_{13}/E_{22} = 0.6,\ G_{23}/E_{22} = 0.5;$$
$$\nu_{12} = \nu_{13} = \nu_{23} = 0.25;\ E_{22} = 10^{06}\text{psi}.$$
$$\alpha_{22}/\alpha_{11} = 2;\ \alpha_{22} = \alpha_{33};\ \alpha_{11} = 1.\times 10^{-06}/^0\text{C},$$

where *E, G,* and ν are Young's modulus, shear modulus and Poisson's ratio. Subscripts 1 and 2 denote the longitudinal and transverse directions, respectively, with respect to the fiber directions at any point in the plane x_1x_2. The layers in the laminate are numbered from the bottom most layers and the fiber-angle is calculated with respect to x_1 axis in an anti-clockwise direction. Layers of equal thickness are considered. The boundary conditions assumed here are as follows:

$$\text{clamped}: u_0 = v_0 = w_0 = \phi_{x_1} = \phi_{x_2} = 0 \text{ at } x_1 = \pm a/2 \text{ and } x_2 = \pm b/2.$$
$$\text{simply supported}: u_0 = w_0 = \phi_{x_2} = 0 \text{ at } x_1 = \pm a/2;\ v_0 = w_0 = \phi_{x_1} = 0 \text{ at } x_2 = \pm b/2$$

TABLE 3. Comparison of mechanical buckling load of a square curvilinear fiber-reinforced composite laminate with different boundary conditions subjected to different loadings (a = b = 254 mm; ply thickness 0.15 mm; $[(\pm(60/15))_4]_s$).

Boundary Conditions	Mechanical Loading Type	Ref. 7 (kN)	Present (kN)
SSSS	Pure Compression (N_{xx})	14.220	14.414
SSSS	Combined Compression – Shear (N_{xx}–N_{xy})	12.070	12.210
CCFF	Pure Compression (N_{xx})	11.652	11.594
SSCC	Combined Compression –Shear (N_{xx}–N_{xy})	20.600	20.540

DOI 10.1002/pc

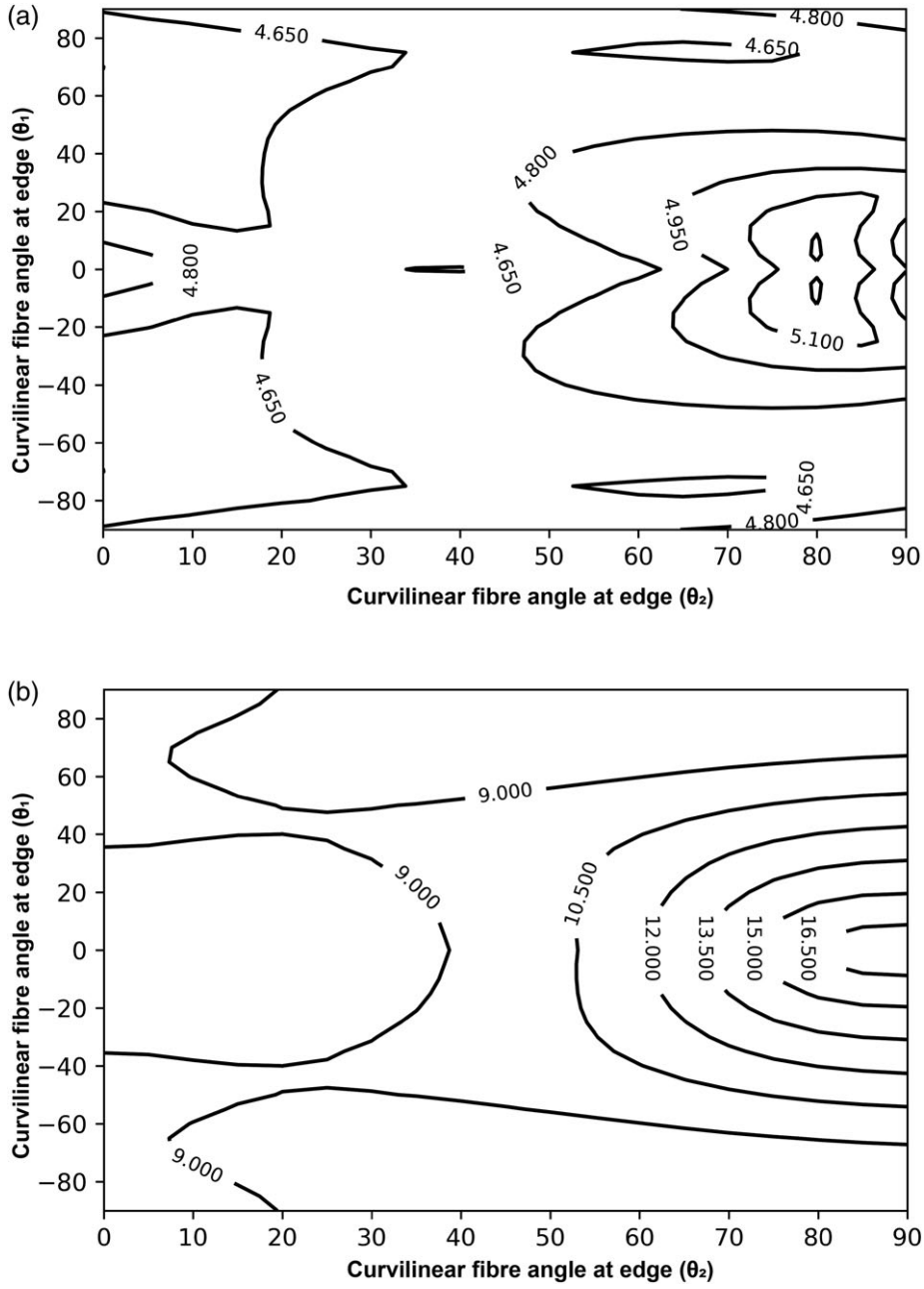

FIG. 3. Contour plot of thermal buckling parameter ($\lambda_{cr}\ \alpha_{11}10^3$) of clamped curvilinear fiber-reinforced composite laminates (a/h = 20, [± (θ_1/θ_2)]2) varying curvilinear fiber angles at the center and edge of the layers.

The thermal environment applied over the laminate for this study is.

Uniform temperature distribution: $T(x_1, x_2) = T_0$.

Non-uniform temperature distribution: (cosine function form) $T(x_1, x_2) = T_0 \cos(\pi x_1/a) \cos(\pi x_2/b)$ $-a/2 < x_1 < a/2$ & $-b/2 < x_2 < b/2$

Initially, the finite element mesh convergence study carried out is depicted in Table 1 considering the thermal buckling of curvilinear fiber-reinforced composite plates subjected to uniform thermal load by assuming eight-layered anti-symmetric square laminates with two thickness ratios and different fiber path angles<$\theta_1\theta_2$>. It is seen from this Table that 8 × 8 mesh provides an acceptable converged result within the tolerance limit of 0.5% for the buckling analysis. Based on the converged mesh, the finite element formulation applied here is further tested considering the thermal bending behavior of straight fiber-reinforced composite laminates with arbitrary boundary conditions (clamped in two opposite edges and simply supported at $x_1 = -a/2$ and $a/2$) and the results given in Table 2 for deflections match very well with the analytical solutions based on higher-order model [48]. However, there is some discrepancy in the stress values due the different approaches used for evaluating the stresses. The shear stresses are obtained in the present analysis using three dimensional elasticity equilibrium equations whereas in

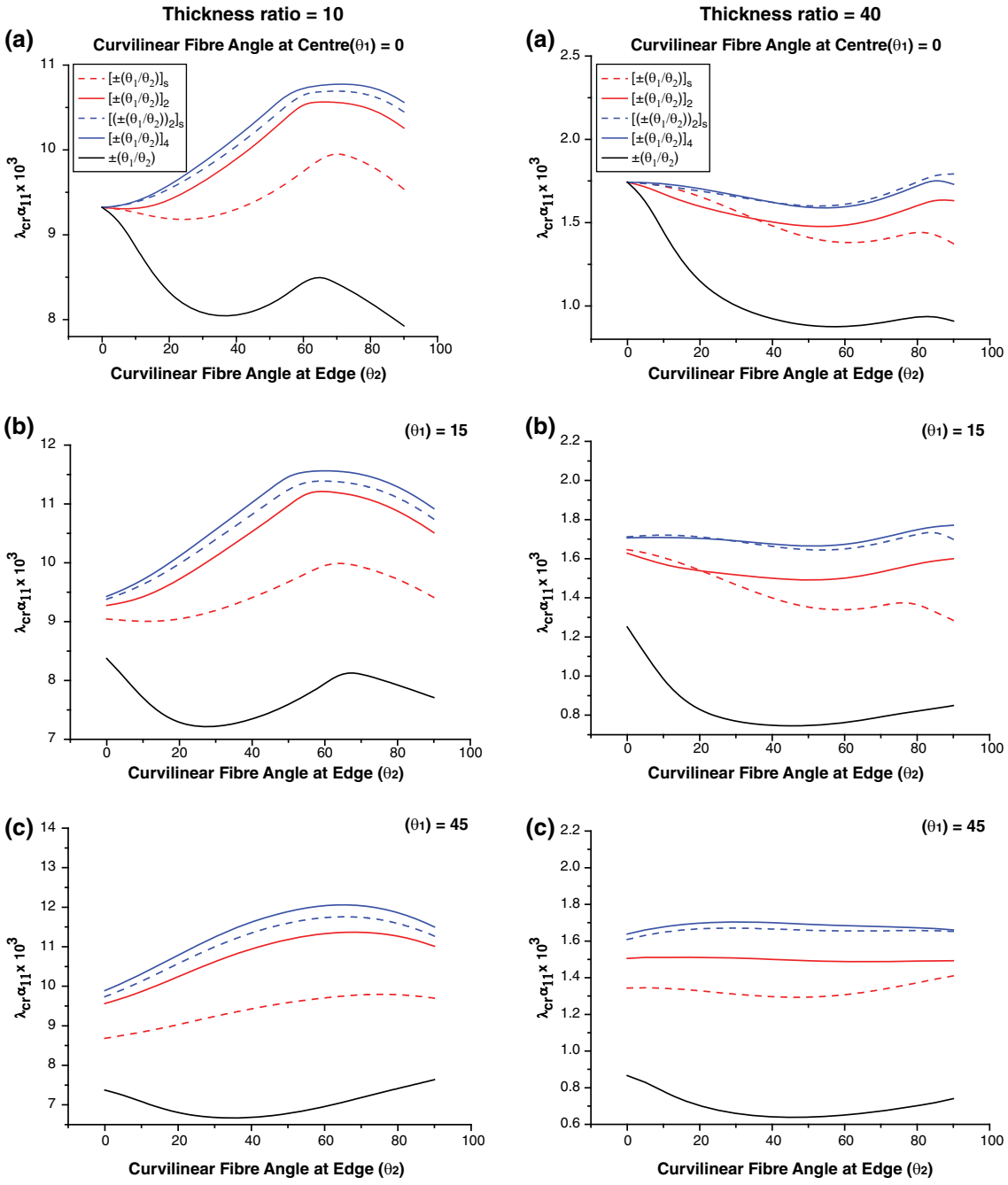

FIG. 4. Critical thermal buckling parameters ($\lambda_{cr}\ \alpha_{11}10^3$) of clamped multi-layered curvilinear fiber-reinforced composite laminates with respect to curvilinear fiber <$\theta_1\ \theta_2$ > lay-ups under uniform thermal load: left side column-a/h = 10; right side column-a/h = 40. [Color figure can be viewed at wileyonlinelibrary.com]

Ref. [48], they are calculated directly using the stress–strain relationship. Also, the critical thermal buckling parameter values obtained for laminates with straight fibers are presented in Fig. 2 assuming different lay-up and ply-angle along with those of available numerical solutions [29] and they are found to be in close agreement.

The thermostructural stability characteristics of curvilinear fiber-reinforced composite laminate under uniform and non-uniform temperature distributions are analyzed varying lay-up and ply-angle. In such composite laminate, the lay-up sequence for symmetric $[\mp(\theta_1/\theta_2)]_s$ is expanded as $\{+(\theta_1/\theta_2), -(\theta_1/\theta_2), -(\theta_1/\theta_2), +(\theta_1/\theta_2)\}$ whereas for anti-symmetric case $[\mp(\theta_1/\theta_2)]_2$ represents$\{+(\theta_1/\theta_2), -(\theta_1/\theta_2), +(\theta_1/\theta_2), -(\theta_1/\theta_2)\}$, respectively. Before proceeding for the thermal stability analysis, the efficacy of the formulation developed here is further checked for the mechanical buckling of curvilinear fiber-reinforced composite plate with different boundary conditions subjected to pure compression, and combined compression-shear loads. The results evaluated here are compared with those of available

 DOI 10.1002/pc

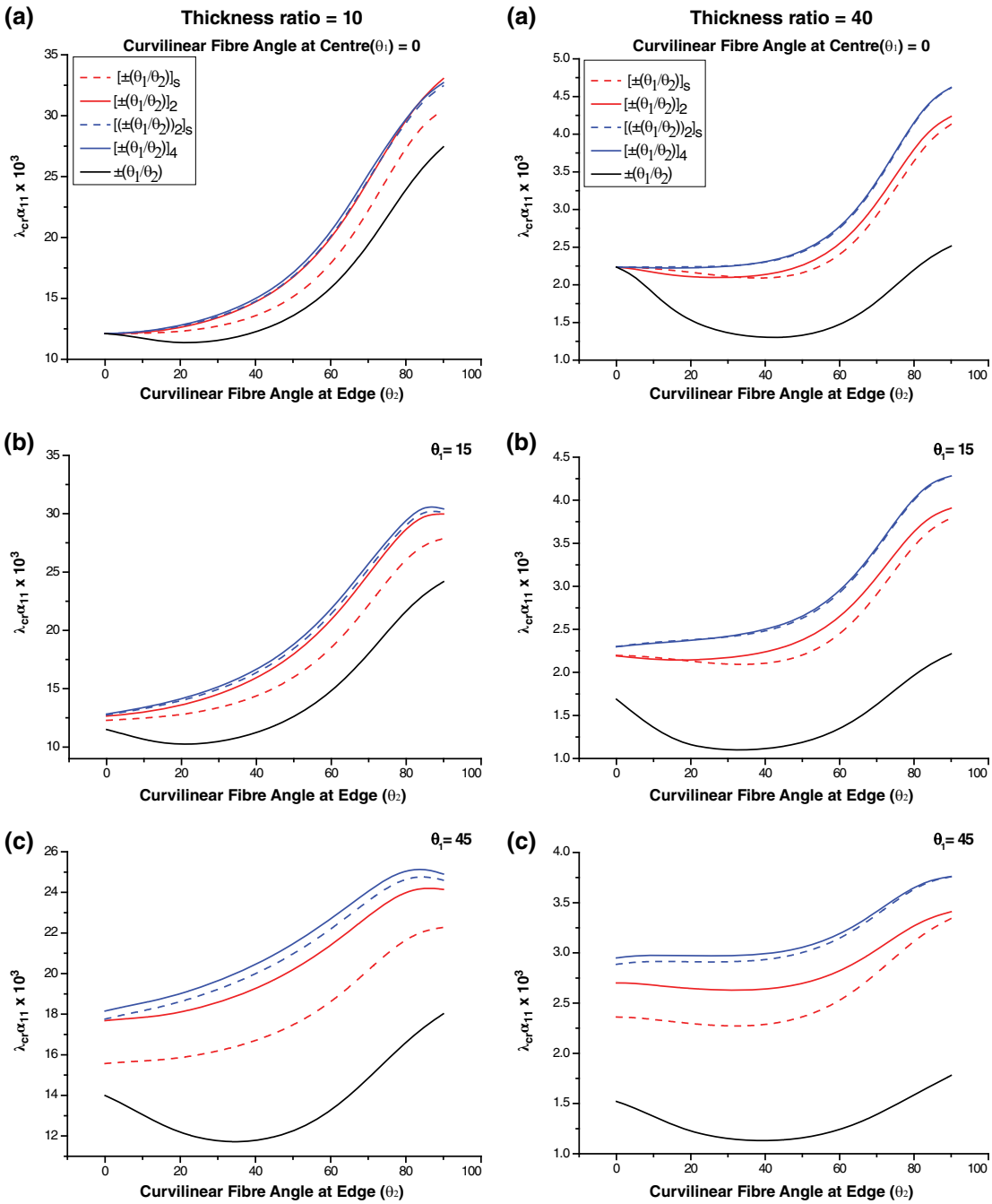

FIG. 5. Critical thermal buckling parameter ($\lambda_{cr}\ \alpha_{11}10^3$) of clamped multi-layered curvilinear fiber-reinforced composite laminates with respect to curvilinear fiber <$\theta_1\ \theta_2$ > lay-ups subjected to non-uniform thermal load: left column-a/h = 10; right column-a/h = 40. [Color figure can be viewed at wileyonlinelibrary.com]

solutions [7] in Table 3 and they are in close agreement. The small discrepancy in the results may be attributed to the different formulations employed in Ref. 7 and in this study. It can be noted that the formulation used in Ref. 7 is based on finite element approach coupled with isogeometric analysis that ensures the continuity of curvilinear fiber angle at any point on the surface whereas the fiber angle varies linearly within the element in the present formulation. A detailed thermal elastic stability study is conducted selecting different values for the fiber angles at the center and edge of the lamina in the laminate. The buckling resisting load contours are shown in Fig. 3 considering four-layered clamped anti-symmetric laminates with uniform and non-uniform thermal distributions. It is viewed from this Figure that the non-dimensional critical buckling temperature parameter ($\lambda_{cr}\alpha_{11}10^3$)with respect to the fiber angle θ_1<40° and θ_2>50° yields higher values. Hence, these ranges for <$\theta_1\theta_2$>are considered as guidelines for carrying out further numerical studies.

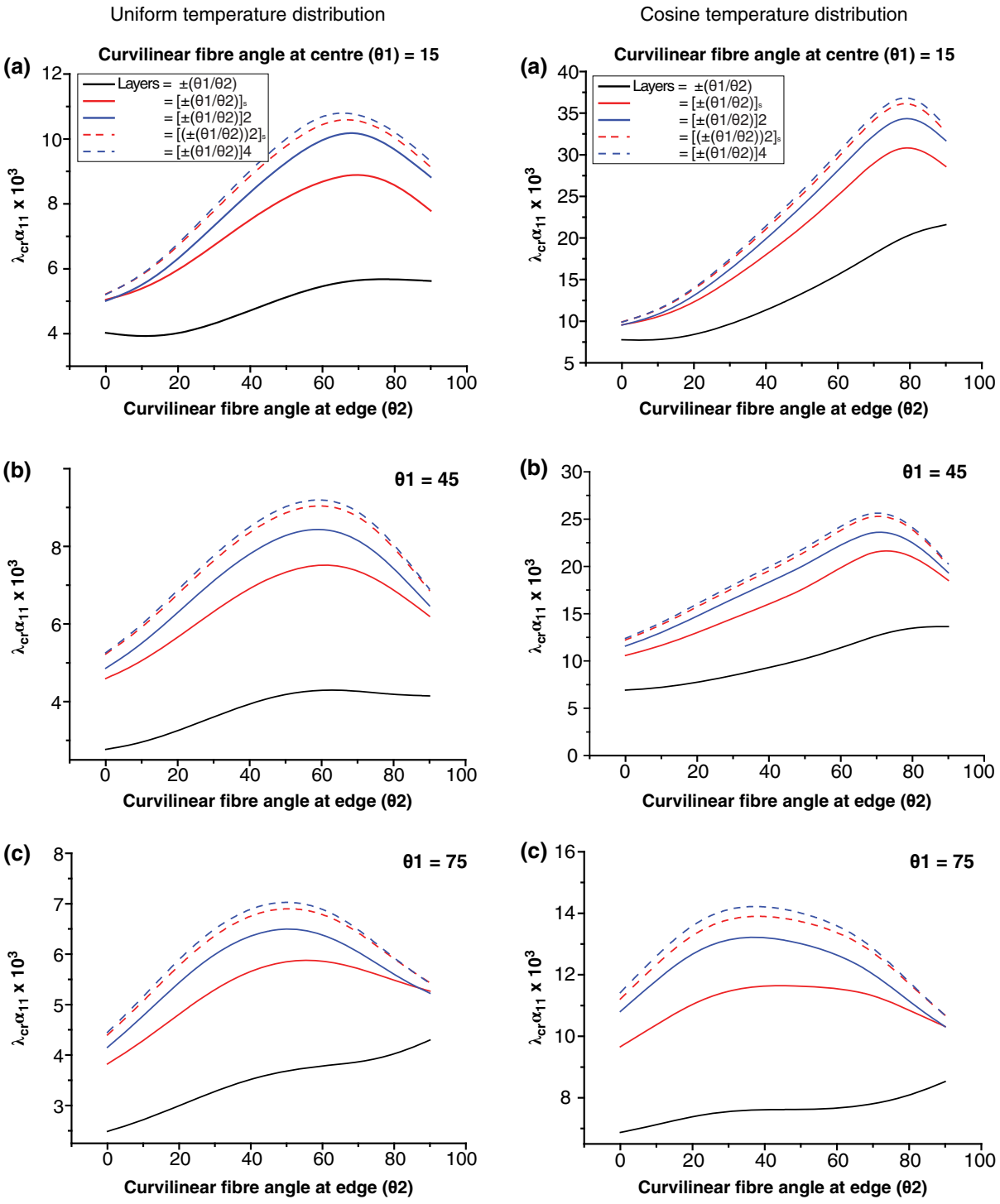

FIG. 6. Critical thermal buckling parameter ($\lambda_{cr}\ \alpha_{11}10^3$) of simply supported multi-layered curvilinear fiber-reinforced composite laminates (a/h = 10) varying lay-up and curvilinear fiber angles $<\theta_1\ \theta_2>$: Left side column: uniform thermal case; Right side column: non-uniform thermal. [Color figure can be viewed at wileyonlinelibrary.com]

Figure 4 presents the non-dimensional critical buckling thermal loads ($\lambda_{cr}\alpha_{11}10^3$) of fairly thick and thin clamped curvilinear fiber composite laminates (symmetric/anti-symmetric) under uniform thermal environment. The fiber angles at the center and edge of the laminate $<\theta_1\theta_2>$are also varied keeping θ_1=0, 15, and 45°, and $\theta_2$changed from 0° up to 90°, respectively. For fairly thick plates (a/h = 10), it is found from Fig. 4 that the anti-symmetric case results in higher buckling temperature for the chosen fiber angle $\theta_1$at the center of the lamina, and it increases with the increase in the fiber edge angle $\theta_2$up to certain value and then decreases. This is attributed to the spatial change

DOI 10.1002/pc

TABLE 4. Critical thermal buckling parameters ($\lambda_{cr}\alpha_{11}10^3$) the four- and eight-layered variable stiffness laminates (a/h = 10 and 20) with SSCC boundary conditions subjected to non-uniform thermal load and by varying curvilinear fiber angles<$\theta_1\theta_2$>.

		Critical Thermal Buckling							
		Four Layer				Eight Layer			
		($\lambda_{cr}\alpha_{11} \times 10^3$)				($\lambda_{cr}\alpha_{11} \times 10^3$)			
		$[\pm(\theta_1/\theta_2)]_s$		$[\pm(\theta_1/\theta_2)]_2$		$[(\pm(\theta_1/\theta_2))_2]_s$		$[\pm(\theta_1/\theta_2)]_4$	
$\theta_1{}^0$	$\theta_2{}^0$	a/h = 10	a/h = 20	a/h = 10	a/h = 20	a/h = 10	a/h = 20	a/h = 10	a/h = 20
15	0	10.383	3.554	10.483	3.52	10.8	3.7067	10.817	3.6963
	15	12.037	4.1459	12.743	4.3482	13.326	4.6781	13.466	4.7159
	40	19.324	7.0977	21.455	7.8691	22.507	8.5642	22.898	8.6973
	45	21.155	7.8924	23.511	8.7216	24.657	9.5102	25.085	9.6493
	60	27.389	10.635	30.113	11.438	31.581	12.546	32.056	12.661
	75	31.554	12.67	34.226	13.223	35.696	14.485	36.16	14.543
	80	31.488	12.769	34.205	13.259	35.484	14.447	35.979	14.501
	90	30.307	12.53	32.965	12.962	33.731	13.878	34.251	13.943
45	0	12.078	4.2177	13.823	4.8901	14.265	5.234	14.591	5.3626
	15	13.918	5.0353	16.236	6.0144	16.931	6.4928	17.36	6.6797
	40	18.129	7.205	21.008	8.4474	21.979	9.1834	22.493	9.4079
	45	18.911	7.6504	21.809	8.8757	22.813	9.6614	23.33	9.8799
	60	21.069	8.9126	23.854	9.9861	24.926	10.906	25.418	11.086
	75	22.466	9.8888	24.939	10.693	25.963	11.671	26.395	11.791
	80	22.595	10.111	24.928	10.801	25.872	11.758	26.282	11.857
	90	22.541	10.453	24.517	10.93	25.212	11.773	25.566	11.836
75	0	13.065	5.7536	14.657	6.6844	14.838	7.0302	15.134	7.2055
	15	14.152	6.4016	15.939	7.325	16.282	7.7815	16.619	7.9504
	40	15.438	7.2966	16.923	7.952	17.424	8.5142	17.697	8.6246
	45	15.562	7.4109	16.946	7.9981	17.465	8.5714	17.718	8.6681
	60	15.811	7.7105	16.875	8.0935	17.42	8.6881	17.613	8.7446
	75	15.995	8.0469	16.72	8.2107	17.223	8.7984	17.356	8.8133
	80	16.041	8.1633	16.654	8.2576	17.119	8.8272	17.233	8.8292
	90	16.124	8.3511	16.553	8.3619	16.899	8.8475	16.982	8.8358
90	0	14.72	7.1569	15.768	7.7386	15.933	8.01	16.129	8.1162
	15	15.473	7.6109	16.598	8.1024	16.828	8.4188	17.044	8.5044
	40	15.976	8.041	16.696	8.2451	16.955	8.5464	17.094	8.577
	45	15.963	8.0765	16.576	8.2282	16.833	8.5152	16.952	8.5367
	60	15.869	8.1762	16.165	8.2032	16.383	8.423	16.443	8.4236
	75	15.821	8.3237	15.883	8.2994	15.993	8.402	16.006	8.3955
	80	15.815	8.3697	15.838	8.3516	15.899	8.4068	15.904	8.4022
	90	15.811	8.4132	15.811	8.4132	15.811	8.4132	15.811	8.4132

in the stiffness over the laminates due to the fiber angle variation over the surface of the laminae. Furthermore, the value of fiber edge angle $\theta_2$corresponding to the maximum critical load depends on the fiber angle at the center of the lamina θ_1. With increase in the fiber angle θ_1, the thermal resisting capacity of the curvilinear laminate increase over the range identified in the contour plot (Fig. 3). The increase in layers further enhances the buckling load as expected. Also, it is seen that the difference in the buckling temperature loads for symmetric and anti-symmetric laminates with 8-layers is less compared with those of two- and four-layered cases. This is due to the reduction in coupling stiffness coefficients due to the presence of bending and stretching coupling with the increase in number of layers. However, the thermal buckling behavior of two-layered case is different in comparison with those of multi-layered cases and it can change significantly over the range of fiber edge angle $\theta_2$and, in particular, while increasing the fiber angle $\theta_1$at the center of the lamina. For thin laminate (a/h = 40) with very low fiber angle $\theta_1$at the center of the lamina, the thermal buckling load initially higher at lowerθ_2 decreases up to certain value of edge fiber angle and then increases to peak value at higher angle θ_2. The maximum critical load corresponds to the fiber angle at the center $\theta_1$around 45° and angle at the edge $\theta_2$around 65° for the parametric study conducted here. The behavior of symmetric or anti-symmetric laminates can noticeably be different for low value of fiber edge angle, in particular, when the number of layers are less. For the non-uniform temperature distribution case, the same clamped laminate is subjected to sinusoidal thermal distribution and the results is described in Fig. 5 with respect to fiber angles <$\theta_1\theta_2$>and for two values of thickness ratio. It is observed from Figure 5 that the maximum critical buckling temperatures occur around $\theta_2$equal to 90°, irrespective of thickness ratio, lay-up and lamina center angleθ_1. Furthermore, it is viewed that the variation of buckling trend is similar for both thick and thin cases unlike in uniform thermal situation. But the

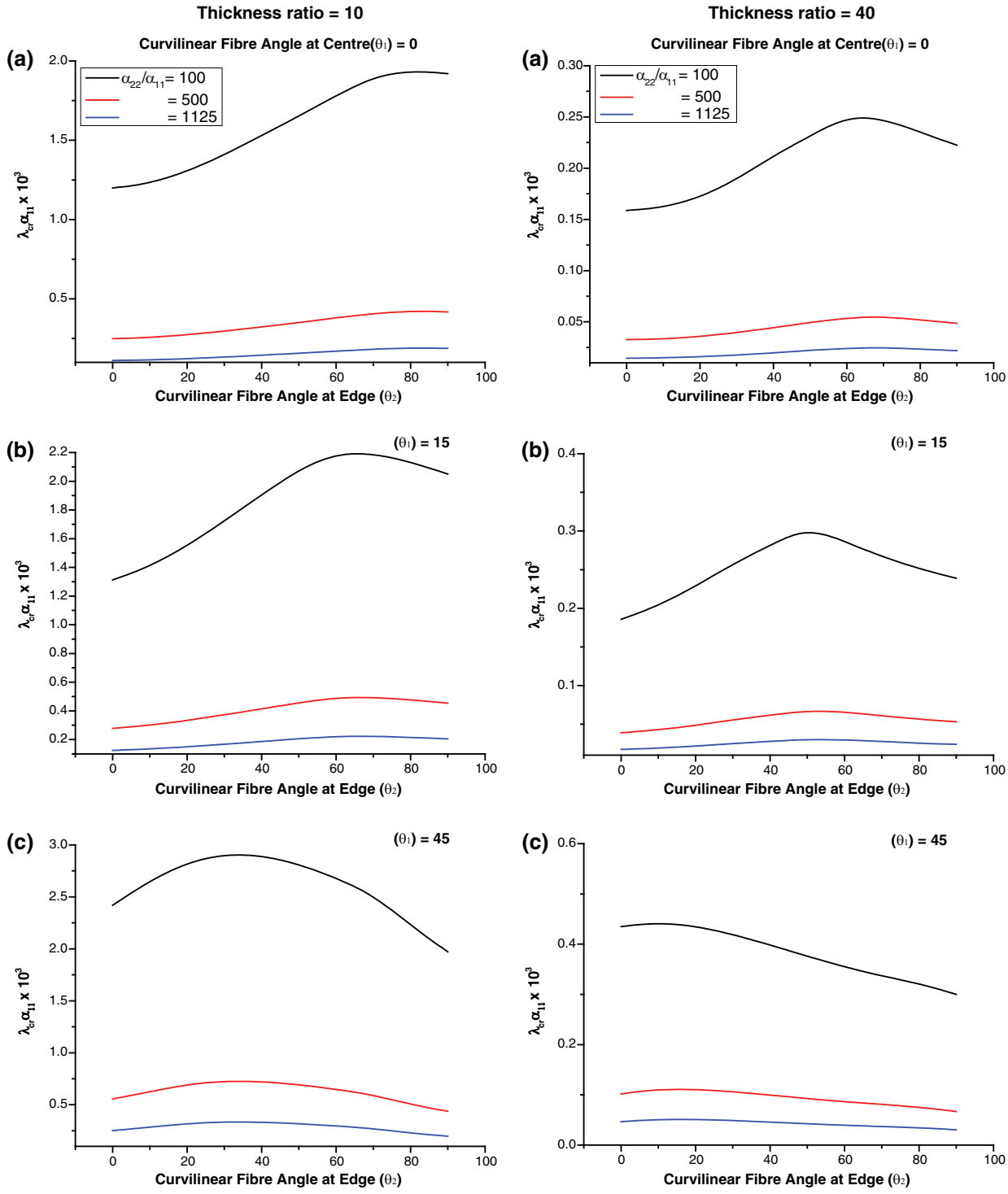

FIG. 7. The influence of thermal coefficient ratios (α_{22}/α_{11}) on the critical thermal buckling parameters (λ_{cr} $\alpha_{11}10^3$) of clamped four-layered curvilinear fiber-reinforced composite laminates ([± (θ_1/θ_2)]2) under uniform thermal load: left column-a/h = 10; right column-a/h = 40. [Color figure can be viewed at wileyonlinelibrary.com]

variation in thermal buckling value with respect to the fiber edge angle $\theta_2$decreases with the increase in the fiber angle $\theta_1$at the center of the laminae.

Next, the effect of other boundary conditions such as simply supported and mixed boundary conditions on the thermal buckling strength is examined and highlighted in Fig. 6 and Table 4, respectively. In Fig. 6, the thermal stability behavior of simply supported curvilinear fiber-reinforced composite laminate with *a/h* = 10 is described by varying the lay-up sequence and ply-angle, respectively. The buckling behavior, in general, is similar to that of clamped case while comparing with Figs. 4 and 5.

DOI 10.1002/pc

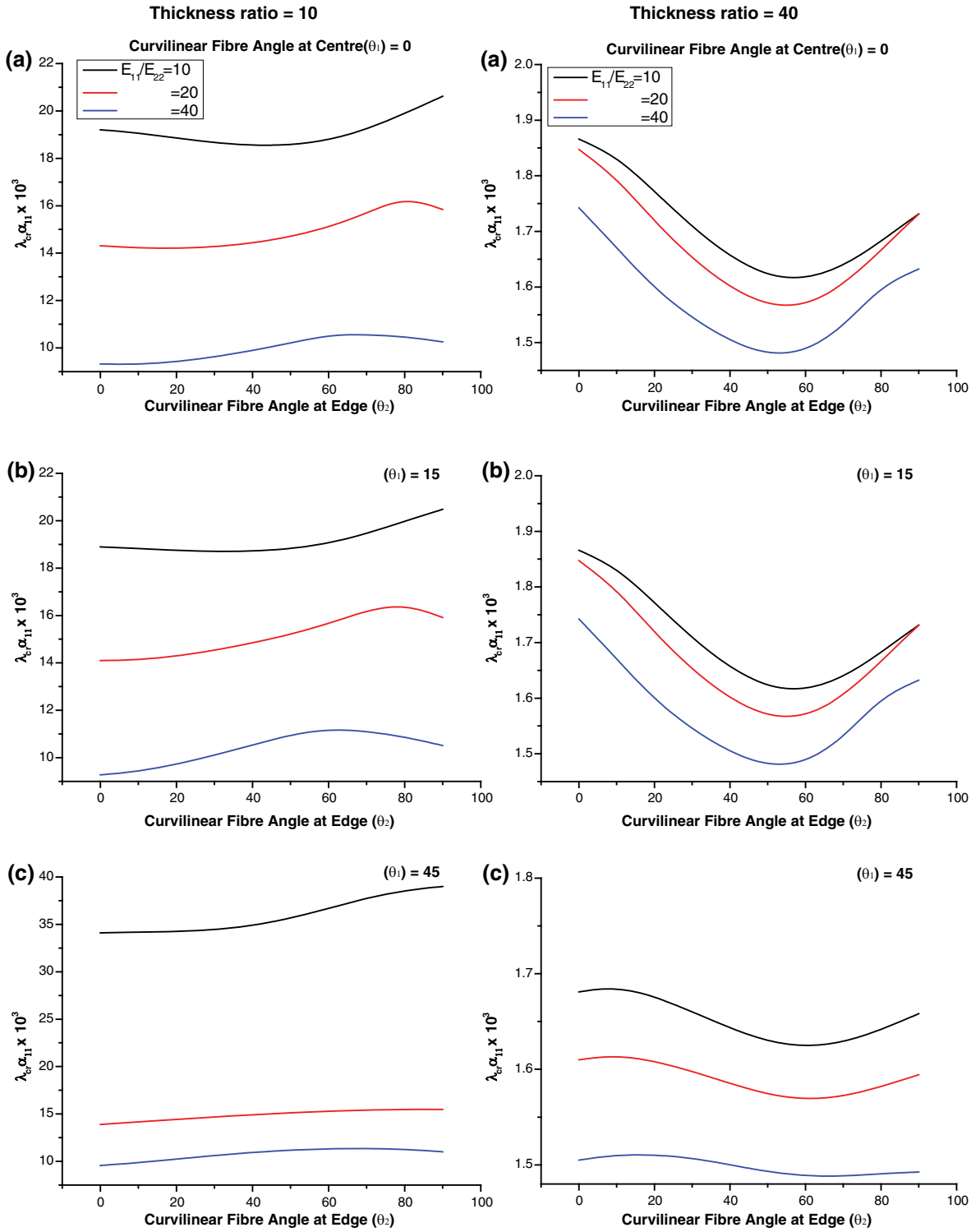

FIG. 8. Critical thermal buckling parameters ($\lambda_{cr}\ \alpha_{11}10^3$) of clamped 4-layered curvilinear fiber-reinforced composite laminates([± (θ_1/θ_2)]2) with respect to modular ratios (E_{11}/E_{22}) under uniform thermal load:left column-a/h = 10; right column-a/h = 40. [Color figure can be viewed at wileyonlinelibrary.com]

However, the actual thermal buckling strength is less for the simply supported case compared with those of clamped one, as expected. The study considering mixed boundary conditions wherein two opposite sides are clamped while the edges $x = -a/2$ and $a/2$ are simply supported (SSCC) is made and the results are shown in Table 4 for laminates with four- and eight-layers (symmetric and anti-symmetric) subjected to non-uniform temperature loading. It is seen from Table 4 and Figs. 4–6 that the buckling resisting strength falls lower than the clamped case but higher than the simply supported one.

Similar study is carried out to see the influence the coefficients of thermal expansion ratio$\alpha_{22}/\alpha_{11}$and modular ratio E_{11}/E_{22} on the thermal buckling parameter of clamped composite laminate with uniform temperature load, by choosing two values for thickness ratio, a/h = 10 and 40. The results are plotted in Figs. 7 and 8 considering curvilinear composite laminate with four-layers and different values for curvilinear fiber angles<$\theta_1\theta_2$>. It is indicated from Fig. 7 that the increase in the coefficients of thermal expansion ratio affects the critical value due to the increase in stress level. However, the variation of buckling temperature with fibers edge angleθ_2 is somewhat different and the fiber edge angle at which maximum critical temperature occurs shifts to lower value with the increase in the fiber angle $\theta_1$at the center of the lamina. Modular ratio E_{11}/E_{22} can also change the elastic stability of curvilinear composite laminate under thermal environment as brought out in Fig. 8. It is seen from Figure 8 that the higher the modular ratio produces lesser critical value and it is similar to the behavior of α_{22}/α_{11}.given in Fig. 7 because of the increase in the thermal stress for the chosen temperature rise.

CONCLUSION

The thermoelastic structural stability of curvilinear fiber-reinforced composite laminates with different boundary conditions is examined using first-order shear deformation theory and considering different types of thermal fields. The formulation takes into account of the spatial variation of fiber angles through the evaluation of the laminate stiffness coefficients. The critical temperatures are predicted using standard eigenvalue procedure. The effect of curvilinear fiber center and edge angles of the lamina, side-to-thickness ratio, lay-up, and coefficient of thermal expansion, and material anisotropy on the critical buckling temperature is examined. It is hoped that the results presented here can be useful in assessing such studies either based on higher-order formulations or other numerical approaches. Some of the salient observations made from this analysis are as follows:

1. For the lower fiber angle at the center, a range of higher angle at the edge of the lamina in the laminate leads to higher critical buckling temperature when dealing with fairly thick laminates.
2. The variation in the buckling temperature value with respect to fiber edge angle of the lamina is somewhat different for thin laminate compared with those of thick case.
3. Thermal buckling load is in general more for anti-symmetric laminate case compared the symmetric laminate.
4. Curvilinear fiber composite laminate with the non-uniform temperature distribution considered here yields higher critical load carrying capacity compared with those of uniformly thermally stressed laminate.
5. Increase in number of layers in the laminate significantly enhances the buckling stability behavior.
6. The thermal stability is significantly affected by the boundary conditions.

Higher the modulus ratio and the thermal expansion coefficient ratio lead to drastically reducing the critical thermal buckling parameter.

7. The qualitative thermal buckling characteristics may change with the combination of continuous change in the laminate stiffness in VSCL and the temperature profile variations.

REFERENCES

1. A.K. Noor and W.S. Burton, *ASME Appl. Mech. Rev.*, **42**, 1 (1989).
2. A.K. Noor and W.S. Burton, *Compos. Struct.*, **14**, 233 (1990).
3. R.K. Kapania and S. Raciti, *AIAA J.*, **27**, 923 (1989).
4. R.K. Kapania, *J. Press. Vessel Technol.*, **111**, 88 (1989).
5. S. Murugan and M.I. Friswell, *Compos. Struct.*, **99**, 69 (2013).
6. M.W. Hyer and H.H. Lee, *Compos. Struct.*, **18**, 239 (1991).
7. P. Hao, X. Yuan, H. Liu, B. Wang, C. Liu, D. Yang, and S. Zhan, *Compos. Struct.*, **165**, 192 (2017).
8. R. Vescovini and L. Dozio, *Compos. Struct.*, **142**, 15 (2016).
9. A. Marouene, R. Boukhili, J. Chen, and A. Yousefpour, *Compos. Struct.*, **139**, 243 (2016).
10. A. Madeo, R.M.J. Groh, G. Zucco, P.M. Weaver, G. Zagari, and R. Zinno, *Thin-walled Struct.*, **110**, 1 (2017).
11. S.C. White, G. Raju, and P.M. Weaver, *J. Mech. Physics Solids*, **71**, 132 (2014).
12. S. Setoodeh, M.M. Abdalla, S.T. Ijsselmuiden, and Z. Gürdal, *Compos. Struct.*, **87**, 109 (2009).
13. H. Ghiasi, K. Fayazbakhsh, D. Pasini, and L. Lessard, *Compos. Struct.*, **93**, 1 (2010).
14. O. Falcó, J.A. Mayugo, C.S. Lopes, N. Gascons, A. Turon, and J. Costa, *Compos. Part B*, **56**, 660 (2014).
15. M.A. Nik, K. Fayazbakhsh, D. Pasini, and L. Lessard, *Compos. Struct.*, **107**, 160 (2014).
16. A. Venkatachari, S. Natarajan, M. Ganapathi, and M. Haboussi, *Compos. Struct.*, **131**, 790 (2015).
17. Z. Wu, G. Raju, and P.M. Weaver, *Int. J. Solid Struct.*, **66**, 132 (2018).
18. A. Venkatachari, S. Natarajan, K. Ramajeyathilagam, and M. Ganapathi, *Compos. Struct.*, **118**, 548 (2014).
19. P. Ribeiro, H. Akhavan, A. Teter, and J. Warmiński, *J. Compos. Mater.*, **48**, 2761 (2014).
20. M.M. Abdalla, S. Setoodeh, and Z. Gürdal, *Compos. Struct.*, **81**, 283 (2007).
21. P. Ribeiro and H. Akhavan, *Compos. Struct.*, **94**, 2424 (2012).
22. A. Houmat, *Compos. Struct.*, **106**, 211 (2013).
23. P. Ribeiro and S. Stoykov, *Compos. Struct.*, **131**, 462 (2015).
24. A. Venkatachari, S. Natarajan, M. Haboussi, and M. Ganapathi, *Compos. Part B*, **88**, 131 (2016).
25. P. Tan and G.J. Nie, *Compos. Struct.*, **149**, 398 (2016).
26. M.A.R. Loja, J.I. Barbosa, and C.M. Mota, *Compos. Struct.*, **182**(402), 402 (2017).
27. T.R. Tauchert, *ASME Appl. Mech. Rev.*, **44**(347), 347 (1991).
28. A.K. Noor and W.S. Burton, *ASME Appl. Mech. Rev.*, **45**, 419 (1992).

29. W.J. Chen, P.D. Lin, and L.W. Chen, *Compos. Struct.*, **41**, 637 (1991).
30. M. Ganapathi and M. Touratier, *Finite Elements in Analysis and Design*, Vol. **28**, 115 (1997).
31. T. Kant and C.S. Babu, *Compos. Struct.*, **49**, 77 (2000).
32. A.R. Vosough, P. Malekzadeh, and M.R. Banan, *Thin-Walled Struct.*, **49**, 913 (2011).
33. D.P. Makhecha, M. Ganapathi, and B.P. Patel, *Compos. Struct.*, **51**, 221 (2001).
34. L.C. Shiau, S.Y. Kuo, and C.Y. Chen, *Compos. Struct.*, **92**, 508 (2010).
35. R. Vescovini, M. D'Ottavio, L. Dozio, and O. Polit, *Compos. Struct.*, **176**, 313 (2017).
36. M. Cetkovic, *Compos. Struct.*, **142**, 238 (2016).
37. M.K. Singha, L.S. Ramachandra, and J.N. Bandyopadhyay, *Compos. Struct.*, **54**, 453 (2001).
38. B.P. Patel, A.V. Lele, M. Ganapathi, S.S. Gupta, and C. T. Sambandam, *Compos. Struct.*, **63**, 11 (2004).
39. B.P. Patel, M. Ganapathi, and D.P. Makhecha, *Compos. Struct.*, **56**(25), 25 (2002).
40. H.-S. Shen, *J. Compos. Mater.*, **47**, 2783 (2013).
41. K.M. Liew, J. Yang, and S. Kitipornchai, *ASME J. Appl. Mech.*, **71**, 839 (2004).
42. R. Javaheri and M.R. Eslami, *AIAA J.*, **40**, 162 (2002).
43. M. Ganapathi and T. Prakash, *Compos. Struct.*, **74**, 247 (2006).
44. T. Prakash, M.K. Singha, and M. Ganapathi, *Eng. Struct.*, **30**, 22 (2008).
45. T. Prakash, N. Sundararajan, and M. Ganapathi, *J. Sound Vib.*, **299**, 36 (2007).
46. T. Yu, T.Q. Bui, S. Yin, D.H. Doan, C.T. Wu, T. Van Do, and S. Tanaka, *Compos. Struct.*, **136**, 684 (2016).
47. F.A. Fazzolari and E. Carrera, *Journal of Thermal Stresses*, **37**, 1449 (2014).
48. A.A. Khdeir and J.N. Reddy, *Journal of Thermal Stresses*, **14**, 419 (1991).
49. T. Kant and R.K. Khare, *Journal of Thermal Stresses*, **17**, 229 (1994).
50. G. Prathap, B.P. Naganarayana, and B.R. Somashekar, *Comput. Struct.*, **29**, 857 (1988).
51. M. Ganapathi, P. Boisse, and D. Solaut, *Int. J. Numer. Method Eng.*, **46**, 943 (1999).
52. R.M. Jones, Mechanics of Composite Materials, McGraw--Hill, New York (1975).
53. O.C. Zienkiewicz and R.L. Taylor, The finite element method, McGraw-Hill, Singapore (1989).